FORMULATION AND CAPTURE OF THE SECOND VOLTAGE PEAK OCCURING FROM PIEZOELECTRIC ENERGY HARVESTING USING A PULSED RESONANT CONVERTER (PRC)

Alex Phipps and Toshikazu Nishida
Electrical and Computer Engineering, University of Florida, USA

Abstract: This paper examines the occurrence of the second voltage peak caused by the pulsed resonant converter (PRC) and investigates the potential advantages of harvesting energy from this additional peak. Analytical expressions are derived which describe the behavior of the second peak and these results are compared to SPICE simulation in order to validate the theoretical models. It is shown that an optimal design point exists when harvesting from both peaks ($\omega\tau$ = 1.76) which is different than the optimal point using only the standard primary peak method ($\omega\tau$ = 1.53).

Keywords: piezoelectric, energy harvesting, pulsed resonant converter

INTRODUCTION

As the number of wireless and portable electronics used in everyday life has increased, interest has grown exponentially in methods that extend the functional lifetime of these systems beyond what batteries alone can provide. Vibration energy harvesting, whereby mechanical vibrations are converted into electrical energy, offers the potential to extend the operational lifetime of these systems indefinitely. Piezoelectric transduction schemes for converting mechanical vibrations into electrical energy are attractive because of their ability to provide moderate power levels (~100uW) at voltages necessary to operate standard electronics (2-10V).

Power converter circuitry is an essential and often overlooked aspect in the design of energy harvesting systems. The role of the power converter is to condition the energy signals and to maximize the amount of harvested power that is delivered to the load. Various power conversion methodologies have been examined for piezoelectric energy harvesting including the rectifier-capacitor [1, 2], synchronized switch harvesting on inductor (SSHI) [3, 4], and synchronized charge extraction (SCE). Of these methodologies, SCE circuits possess the advantage of operating independently of their load and therefore not requiring additional DC-DC conversion and the associated inductive components. The pulsed resonant converter (PRC) is a SCE topology that utilizes a single, minimally-sized inductor and two switches to extract energy from the piezoelectric transducer.

A schematic model of a PRC-based piezoelectric energy harvesting system is shown in Fig. 1. The input to the PRC is the piezoelectric transducer which converts mechanical energy into electrical energy. The transducer is modeled as a sinusoidal current source (representing an oscillating vibration source) in parallel with the piezoelectric capacitance, C_{piezo}, and a parallel leakage term, R_{piezo}. This model is typically valid if the electromechanical coupling of the transducer is low. The load of the PRC is a rechargeable battery or super-capacitor.

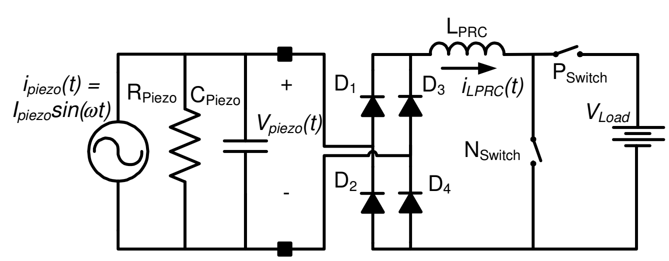

Fig. 1: Circuit representation of the transducer and PRC.

For standard operation, the PRC transfers energy accumulated on the piezoelectric capacitance to the load when the magnitude of the piezoelectric voltage is at a maximum, as shown in Fig. 2. The rectifier allows energy to be harvested from this primary voltage peak twice every vibration period. However, as a result of the non-linear switching behavior of the PRC, a secondary voltage wave is created which can be harvested at its peak to provide additional energy to the system. Previous works employing the PRC have focused primarily on its circuit implementation [5, 6]. These works show the occurrence of the secondary wave in both simulation [5] and in experimental results [6], but have not attempted to describe or model this behavior.

In order to effectively design and optimize PRC-based energy harvesting systems for maximum power collection, accurate modeling of the secondary wave is necessary. This paper presents a detailed examination of the secondary wave behavior, and demonstrates how harvesting the secondary wave increases the total harvested power collected by the system.

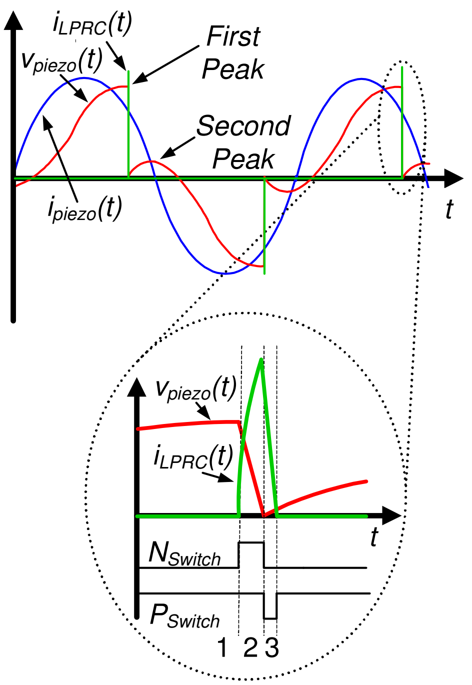

Fig. 2: Current and voltage waveforms for energy harvesting using the PRC.

OPERATION OF THE PRC

Standard operation

The basic operation of the PRC is divided into three phases, 1-3, as shown in Fig. 2. During phase 1, both the N_{Switch} and P_{Switch} are open, and the piezoelectric voltage, $v_{piezo}(t)$, ramps up sinusoidally as charge accumulates on C_{piezo}. Phase 1 is designed to be much longer than the other two phases, and therefore the piezoelectric transducer is open-circuited for a majority of its operation. When $v_{piezo}(t)$ reaches its maximum value, corresponding to a maximum amount of energy stored on C_{piezo} ($E = ½ CV^2$), phase 2 begins and N_{Switch} closes. An LC resonant circuit is formed between C_{piezo} and L_{PRC}, and harvested energy stored on C_{piezo} is transferred to the inductor. The inductor current, $i_{LPRC}(t)$, rises sinusoidally as $v_{piezo}(t)$ falls to zero. Phase 3 begins when all of the energy has been transferred to L_{PRC}, which is marked by $v_{piezo}(t)$ reaching zero and $i_{LPRC}(t)$ reaching its maximum value. During phase 3, N_{Switch} is opened and P_{Switch} is closed. The energy stored on L_{PRC} is transferred to the load until $i_{LPRC}(t)$ reaches zero, at which point P_{Switch} opens, and the PRC returns to phase 1.

For an ideal PRC with zero losses, the power delivered to the load is equal to the energy stored on C_{piezo} at the end of phase 1 given by

$$P_{PRC} = E_{Cpiezo} f_{sw} = \frac{1}{2} C_{piezo} V_{PRC}{}^2 f_{sw}\,, \tag{1}$$

where f_{sw} is twice the vibration frequency (due to rectification of $v_{piezo}(t)$ by diodes D_1-D_4) and V_{PRC} is the maximum piezoelectric voltage at the end of phase 1. Under steady-state conditions, V_{PRC} is given by

$$V_{PRC} = \frac{I_{piezo}\tau}{C_{piezo}\sqrt{1+\omega^2\tau^2}}\left(1+e^{\frac{-\pi}{\omega\tau}}\right), \tag{2}$$

where $\tau = C_{piezo} R_{piezo}$ and ω is the vibration frequency of the transducer. Combining (1) and (2), the power from the first peak of the PRC is given as [7]

$$P_{PRC} = \frac{I_{piezo}{}^2 R_{piezo}}{2\pi}\,\frac{\omega\tau}{1+\omega^2\tau^2}\left(1+\mathrm{e}^{\frac{-\pi}{\omega\tau}}\right)^2. \tag{3}$$

Occurrence of the 2^nd^ Wave

The occurrence of the secondary wave in the piezoelectric voltage results from the combination of the phase shift between $v_{piezo}(t)$ and $i_{piezo}(t)$ and the non-linear switching behavior of the PRC. When $v_{piezo}(t)$ is at its maximum amplitude, the PRC extracts the harvested energy and delivers it to the load almost instantaneously relative to the vibration period. As a result of this extraction, $v_{piezo}(t)$ is reduced to zero volts. However, immediately following the extraction, the current source $i_{piezo}(t)$ is nonzero as shown in Fig. 2. Since the transducer is now operating in phase 1, $i_{piezo}(t)$ again charges C_{piezo} resulting in the secondary wave. This secondary voltage waveform can be described analytically by the equation

$$v_{piezo}(t) = \frac{I_{piezo}\tau}{C_{eb}\sqrt{1+\omega^2\tau^2}}\left(\cos(\omega t) - e^{\frac{-t}{\tau}}\right), \tag{4}$$

where t=0 is defined at the beginning of the 2^nd^ phase 1. A complete derivation of (4) is presented in Appendix A.

Unlike the value of the first voltage peak given in (2) which can be found explicitly, an implicit numerical solution is required to obtain the peak value of the secondary wave given in (4).

VALIDATION OF THE THEORETICAL MODEL USING SPICE SIMULATION

SPICE simulation (LTSPICE IV from Linear Technology) was used to validate the theoretical models of the secondary voltage wave behavior of $v_{piezo}(t)$. Figure 3 shows the secondary peak value of $v_{piezo}(t)$, both analytically using (4) and via SPICE simulation, as a function of R_{piezo} and C_{piezo} for typical values encountered in piezoelectric transducers. It can be seen that higher piezoelectric voltages occur for lower values of C_{piezo} and higher values of R_{piezo}. This behavior can be best explained considering that $i_{piezo}(t)$ is fixed for this data, since small values of C_{piezo} charge to higher voltages and large values of R_{piezo} suffer less leakage.

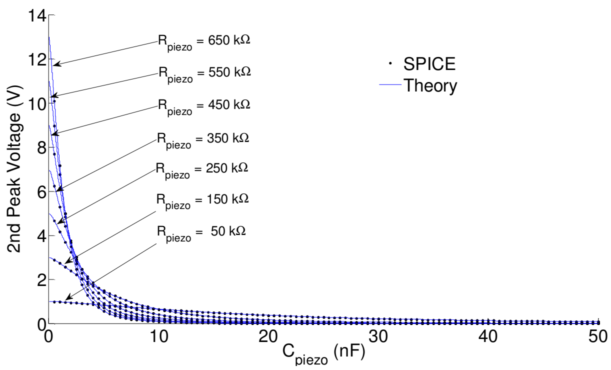

Fig. 3: Maximum voltage values of the second peak.

The maximum power available from the secondary voltage wave is shown in Fig. 4 using (1) and the peak voltage of the secondary wave in (4). For each value of R_{piezo}, an optimal value of C_{piezo} exists where the power from the secondary peak is maximized.

PRC DESIGN USING THE SECOND PEAK

The goal of harvesting energy from the secondary peak is to increase the total power collected by the harvesting system. In order to design a system which does this effectively, it is necessary to understand how the design parameters affect the total harvested power.

Consider first the effect that harvesting the secondary peak has on the total power harvested by the system. Figure 5 compares the total power obtained from harvesting ***only*** the primary peak to the power produced by harvesting from both the primary ***and*** secondary peaks. An optimal point exists for each case corresponding to a specific value of the product of $\omega\tau$ where the harvested power is maximized ($\omega\tau$=1.76 for the primary only case and $\omega\tau$=1.53 for both). From these results, it can be seen that, at their respective optimal points, the power harvested from both peaks is greater than that harvested from only the first peak.

The secondary wave behavior of $v_{piezo}(t)$ has been presented for PRC-based energy harvesting systems. Equations characterizing both the voltage and harvestable power have been developed and validated through SPICE simulation. Through the careful design of transducer parameters, these systems can be designed for increased performance by utilizing the second peak. While this work focuses on the characterization of the secondary voltage peak, it is possible to imagine a system where additional peaks (third, fourth, etc…) exist as a result of the PRC operation. A future goal of this research is to characterize an optimal design point for a system with N additional peaks in order to further increase the total harvested power.

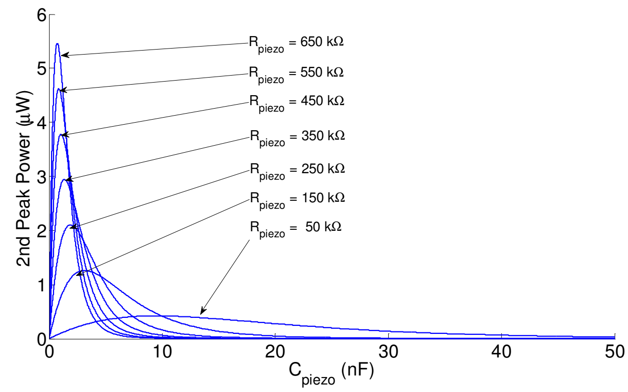

Fig. 4: Maximum power from the second peak.

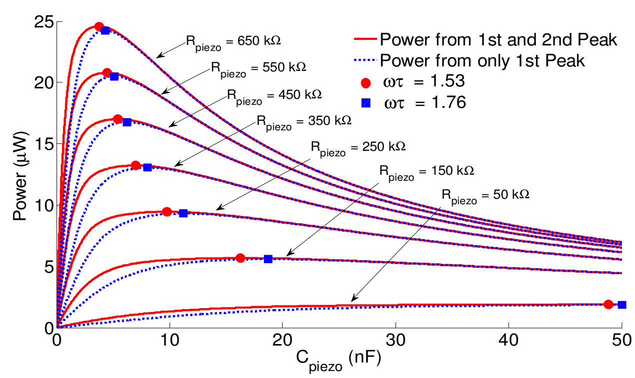

Fig 5: A comparison of power from only the 1st peak vs. the combined power from 1st and 2nd peaks.

REFERENCES

[1] Ottman G, Hoffman H, Bhatt A, Lesieutre G 2002 Adaptive piezoelectric energy harvesting circuit for wireless remote power supply *IEEE Trans. Power Electron.* **17** 669-676

[2] Ottman G, Hoffman H, Lesieutre G, 2003 Optimized piezoelectric energy harvesting circuit using step-down converter in

discontinuous conduction mode *IEEE Trans. Power Electron.* **18** 696-703
[3] Badel A, Benayad A, Lefeuvre E, Lebrun L, Richard C, Guyomar D 2006 Single crystals and nonlinear process for outstanding vibration-powered electrical generators *IEEE Trans. Ultrason., Ferroelectr., Freq. Control* **53** 673-684
[4] Guyomar D, Badel A, Lefeurve E, Richard C 2005 Toward energy harvesting using active materials and conversion improvement by nonlinear processing *IEEE Trans. Ultrason., Ferroelectr., Freq. Control* **52**, 584-595
[5] Hehn T, Peters C, Hagedorn F, Ortmanns M, Manoli Y 2008 A CMOS Integrated Interface for Piezoelectric Generators *Technical Digest PowerMEMS 2008 (Sendai, Japan 9-12 November 2008)* 457-460
[6] Xu S, Ngo K, Nishida T, Chung G, Sharma A 2007 Low frequency pulsed resonant converter for energy harvesting *IEEE Trans. Power Electron.* **22** 63-68
[7] Ngo K, Phipps A, Nishida N, Lin J, Xu S 2006 Power Converters for Piezoelectric Energy Extraction *Proceedings of ASME International Mechanical Engineering Congress and Exposition 2006 (Chicago, IL 5-10 November 2006)*

APPENDIX A

Derivation of $v_{piezo}(t)$ during the secondary wave

After the occurrence of the first peak and the associated extraction of energy, both the N_{Switch} and P_{Switch} are off, and the transducer operates in open circuit mode. Using Kirchoff's Current Law, the behaviour of the transducer can be described by

$$I_{piezo}\sin(\omega t+\phi)=\frac{v_{piezo}(t)}{R}+C\frac{dv_{piezo}(t)}{dt}, \tag{5}$$

where $\phi=\pi/2+\tan^{-1}(\omega\tau)$ is the phase shift between $v_{piezo}(t)$ and $i_{piezo}(t)$. The total solution to the differential equation in (5) is the sum of the homogeneous and particular solutions given by

$$v_{piezo}(t)=ke^{\frac{-t}{\tau}}+A\cos(\omega t+\phi)+B\sin(\omega t+\phi), \tag{6}$$

where k is an integration constant, and A and B are

$$A=-\frac{I_{piezo}\omega\tau^2}{C_{piezo}\left(1+\omega^2\tau^2\right)}$$
$$B=\frac{I_{piezo}\tau}{C_{piezo}\left(1+\omega^2\tau^2\right)}. \tag{7}$$

Assuming that the PRC is operating in steady-state and the waveforms in Fig. 2 are periodic, the beginning of the second wave can be designated as $t=0$. The integration constant k is then found to be

$$k=\frac{I_{piezo}\tau}{C_{piezo}\left(1+\omega^2\tau^2\right)}\left[\omega\tau\cos(\phi)-\sin(\phi)\right] \tag{8}$$

using the initial condition

$$v_{piezo}(0)=0. \tag{9}$$

The total solution of $v_{piezo}(t)$ then becomes

$$v_{piezo}(t)=\frac{I_{piezo}\tau}{C_{eb}\left(1+\omega^2\tau^2\right)}\Big[-\omega\tau\cos(\omega t+\phi)+\sin(\omega t+\phi)+\left(\omega\tau\cos(\phi)-\sin(\phi)\right)e^{-t/\tau}\Big]. \tag{10}$$

Substituting in the value of ϕ and simplifying terms, it can be found that for the secondary wave

$$v_{piezo}(t)=\frac{I_{piezo}\tau}{C_{eb}\sqrt{1+\omega^2\tau^2}}\left(\cos(\omega t)-e^{\frac{-t}{\tau}}\right). \tag{11}$$